Network Based Approaches to Detection of Geodetic Transients Final Report 2012

Paul Segall
Stanford University Geophysics Department

Collaborators: Junichi Fukuda (E.R.I University of Tokyo), Jeff McGuire (WHOI), Jessica Murray-Moraleda (USGS)

February 26, 2012

1 Summary

We worked on two inter-related approaches for detection of transient deformation. The fundamental assumption in both is that transient tectonic deformations are spatially coherent and can thus be separated from localized errors. If not required by the data, fault slip-rate or strain-rate is assumed to be steady in time.

The first approach is an extension of the Network Inversion Filter (NIF) known as a Monte Carlo mixture Kalman Filter (MCMKF). The NIF estimates spatially and temporally variable fault slip-rates in the presence of various noise sources. Elastic Green's functions impose spatial coherence on the deformation. The NIF included a constant temporal smoothing parameter (α^2). The MCMKF, however, propagates a discrete probability density of α^2 that changes with time. When the data reflect steady-state deformation α^2 is small (strong smoothing); however during transient slip larger values of α^2 are favored. The integrated probability of α^2 over a specified threshold is thus a measure of the probability that a transient has occurred.

We also developed a Network Strain Filter (NSF) that seeks coherent transients in the surface strain-rate field. This approach is not dependent on a particular fault model. The two approaches, NIF and NSF, are complementary, in that the NSF may first detect transients, which could be further analyzed with a NIF. In both cases spatial coherence is enforced on the transient signal at the outset. This contrasts with other approaches that analyze station time individually, and then look to see if the deviations from steady-state are spatially coherent.

2 Technical Report

We now have deformation measurements that are sufficiently dense in space and time to motivate the development of methods for online detection of deformation transients. To date, several algorithms have been utilized to detect and analyze transient deformation. The Network Inversion Filter (NIF) [*Segall and Matthews*, 1997; *McGuire and Segall*, 2003] and Network Strain Filter (NSF) [*Ohtani et al.*, 2010] can be used to estimate spatio-temporal variations in fault slip rate (NIF), or strain-rate (NSF), from geodetic data. The fundamental assumption in both algorithms is that transient tectonic displacements are spatially coherent and can thus be separated from localized error sources. If not required by the data, fault slip rate or strain rate is steady in time.

A challenge for all transient detection methods is assigning a significance level to potential anomalies. Finding possible transients is not difficult – determining whether they are statistically significant is more difficult. A particular limitation of the NIF and NSF is that a smoothing parameter that governs temporal variations in slip or strain is assumed to be constant in time. This can lead to under or oversmoothed temporal variations. An oversmoothed estimate could lead to a delayed real-time detection or possibly a failure to detect, because the modeled transient will evolve more slowly than the actual transient. On the other hand, an under smoothed estimate could lead to time-series noise being mapped into signal.

Fukuda et al. [2004; 2008] overcome this with the implementation of a particle filter, referred to as a Monte Carlo mixture Kalman Filter (MCMKF), that allows for rapid changes in temporal smoothing. The MCMKF propagates a discrete probability distribution of the temporal smoothing parameter sequentially in time. When the data reflect steady-state deformation, the smoothing parameter tends toward a low value (strong smoothing). However, if the data reflect transient fault slip or strain, larger values of smoothing parameter (weak smoothing) are favored. Although this method was designed for retrospective detection and imaging of past transients, the approach lends itself directly to a true on-line, real-time transient detector.

2.1 Fault Slip Transient Detection

The MCMKF employs the forward model used in the NIF [*Segall and Matthews*, 1997]. Displacement as a function of position $\mathbf{x}$ and time t, $\mathbf{u}(\mathbf{x},t)$, is modeled as the sum of contributions from fault slip, local benchmark motion, reference frame, and measurement errors,

$$\mathbf{u}(\mathbf{x},t) = \int_A \mathbf{G}(\mathbf{x},\boldsymbol{\xi})\mathbf{s}(\boldsymbol{\xi},t)d\boldsymbol{\xi} + \mathcal{L}(\mathbf{x},t) + \mathbf{F}\mathbf{f}(t) + \mathbf{e}. \tag{1}$$

The first term on the rhs of (1) represents the displacement due to slip $\mathbf{s}(\boldsymbol{\xi},t)$ on fault in an elastic half space, where $\mathbf{G}(\mathbf{x},\boldsymbol{\xi})$ is the elastostatic Green's function. The second term $\mathcal{L}(\mathbf{x},t)$ represents colored noise due to random benchmark motions. The third term $\mathbf{F}\mathbf{f}(t)$ represents reference frame errors, where $\mathbf{F}$ is a Helmert transformation matrix and $\mathbf{f}(t)$ is a vector of rigid body translation, rotation, and scale factor. Fault slip $s_p(\boldsymbol{\xi},t)$, is expanded in M spatial basis functions $B_k^{(p)}(\boldsymbol{\xi})$ as $s_p(\boldsymbol{\xi},t) = \sum_{k=1}^{M} c_k(t)B_k^{(p)}(\boldsymbol{\xi})$ where $c_k(t)$ are temporally varying coefficients. [*Segall et al.*, 2000; *Fukuda et al.*, 2008]. Differentiating with respect to time, yields slip rate $\dot{s}_p(\boldsymbol{\xi},t)$ in terms of the coefficients, $\dot{c}_k(t)$. The slip-rate coefficients, $\dot{c}_k(t)$, are modeled as random walk processes with scale parameter α

$$\dot{c}_k(t_n) = \dot{c}_k(t_{n-1}) + v_n^{(k)}, \qquad v_n^{(k)} \sim N\left(0, \alpha^2 \Delta t_n\right) \tag{2}$$

where $v_n^{(k)}$ is the process noise and Δt_n is the time interval. From (2) a low value of α^2 yields strong temporal smoothing, whereas larger values of α^2 are required to capture rapid changes in slip-rate. Therefore, α^2 can be regarded as a temporal smoothing parameter.

Fukuda et al. [2004, 2008] introduced a time-varying smoothing parameter, $\alpha^2(t)$. They implemented a Bayesian sequential filtering algorithm referred to as a Monte Carlo mixture Kalman filter (MCMKF) that combines a particle filter and the Kalman filter to estimate joint posterior pdf of $\alpha^2(t)$ and the state vector. The MCMKF consists of two steps. First, the temporal evolution of the posterior pdf of $\alpha^2(t)$ is obtained using a particle filter [*Kitagawa*, 1996; *Fukuda et al.*, 2004]. Second, the temporal evolution of the state vector (including the slip distribution) is estimated using $\alpha^2(t)$ obtained in the first step. Let α_k^2 denote $\alpha^2(t_k)$ and let $\mathbf{d}_k$ be data observed at time t_k. The posterior probability distribution of $\alpha_1^2, \alpha_2^2, \ldots, \alpha_n^2$ conditioned on data $\mathbf{d}_1, \mathbf{d}_2, \ldots, \mathbf{d}_n$, $p(\alpha_1^2, \ldots, \alpha_n^2 | \mathbf{d}_1, \ldots, \mathbf{d}_n)$, can be obtained through prediction and filtering steps, as in a standard Kalman Filter.

The algorithm is suitable for online transient detection for two reasons. First, it is recursive; the posterior distribution of α_{n-1}^2 is updated to generate the distribution of α_n^2. Second, from the posterior probability distribution of $\alpha^2(t)$, we can quantify the statistical significance of a transient event as shown below.

The method applied to a a simulated transient (Figure 1) illustrates the method. Figure 1(b) shows the the input slip-rate. Figure 1(a) shows the estimated posterior probability distribution of $\alpha^2(t)$. Note that $\alpha^2(t)$ is distributed over smaller values while slip rate is constant. However, when the slip rate rapidly changes, $\alpha^2(t)$ concentrates on larger values.

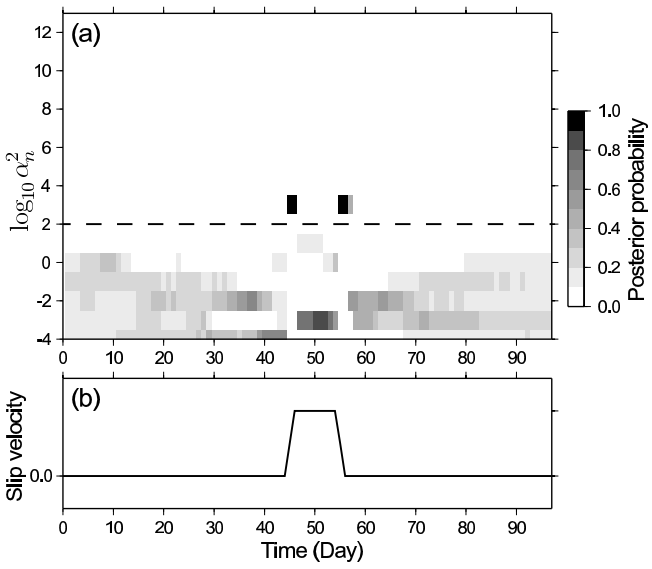

Figure 1: (a) Estimated temporal variation of posterior pdf of $\alpha^2(t)$, in a simulation. Dashed line shows the maximum likelihood estimate for constant α^2, as in the original NIF. (b) Time dependence of true slip velocity on the transient slip patch. *Fukuda et al.* [2008].

For $\alpha^2(t)$ below some threshold value, the system is effectively at steady-state. We thus define a threshold value, $\alpha_{\min}^2$, such that if $\alpha^2(t) < \alpha_{\min}^2$, slip rate is regarded as in a steady-state whereas if $\alpha^2(t) > \alpha_{\min}^2$ a transient is in progress. Using the threshold value $\alpha_{\min}^2$, one can compute the probability that the system is no longer steady-state at time t_k, $p_{\text{transient}}(t_k)$,

$$p_{\text{transient}}(t_k) = p(\alpha_k^2 > \alpha_{\min}^2 | \mathbf{d}_1, \mathbf{d}_2, \ldots, \mathbf{d}_n) \qquad = \int_{\alpha_k^2 > \alpha_{\min}^2} p(\alpha_k^2 | \mathbf{d}_1, \mathbf{d}_2, \ldots, \mathbf{d}_n) d\alpha_k^2, \qquad (3)$$

for $k = 1, 2, \ldots, n$. This provides a measure of the probability that a transient slip-rate change has been detected at the specified level.

The transient detection algorithm proceeds as follows. We run the MCMKF algorithm to estimate the posterior probability distribution of $\alpha^2(t)$. At each epoch, we calculate the probability using the posterior distribution obtained by the filtering algorithm. If the probability given by equation (3) exceeds some threshold, we consider a transient to be detected.

We illustrate the MCMKF on a slow slip event in the Boso Peninsula region of Japan in 2002. Figure 2 shows daily GPS time series at three selected stations. Rapid transient displacements were observed between day of year (DOY) 276–285, and the transient continued after DOY 285 with smaller displacement rates. Figure 3 shows evolution of $p_{\text{transient}}(t_k) = p(\alpha_k^2 > \alpha_{\min}^2 | \mathbf{d}_1, \mathbf{d}_2, \ldots, \mathbf{d}_n)$ with time.

The filter starts at day 240 and it appears initially that there is a possibility of a transient (with data only up to the present it is difficult to know if today is the start of a transient), however as more data are collected it becomes clear there is no transient there. The actual transient that starts near day 276 shows up very clearly and becomes pronounced as more data are collected. In this case the occurrence of a transient is detected with high confidence. Other synthetic tests show that subtle transients require more data and are detected at a lower confidence level.

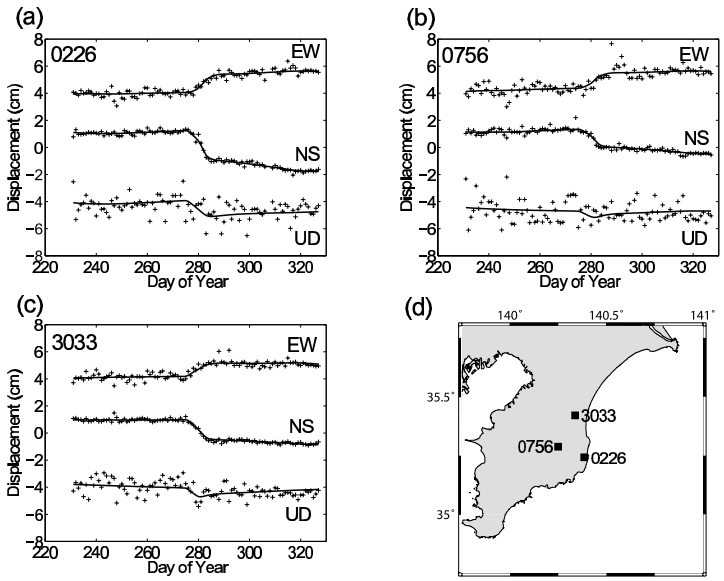

Figure 2: 2002 Boso Japan slow slip event. Observed and computed displacements at 3 stations. Solid lines show predicted displacements. (d) Locations of the selected stations.

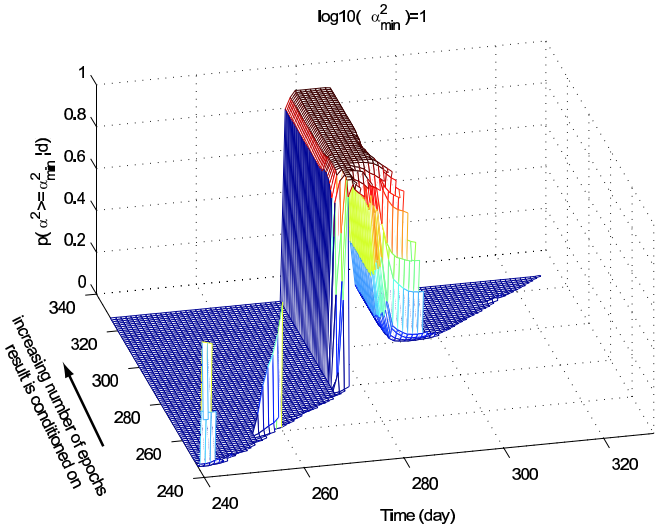

Figure 3: Mesh plot showing the probability $p_{\text{transient}}(t_k)$ the probability that the acceleration parameter $\alpha^2(t)$ exceeds the threshold, $\log_{10} \alpha_{\min}^2 = 1$, given data up to epoch n. Time t_k is shown on the right axis, and the current time t_n is shown on the left axis. Note that at the current day t_n, $\alpha^2(t)$ can only be conditional on data up to that day, so that $k \leq n$, hence there is mesh only for the "back triangle".

The detection algorithm involves internal parameters that influence $p_{\text{transient}}(t)$, These include parameters that control spatial smoothing, the transition probability in the particle prediction step (as discussed in *Fukuda et al.* [2004, 2008]), as well as the filter "lag", defined as follows. In principal, the estimate of α^2 at all past epochs is updated with every new observation. However, *Kitagawa* [1996] showed that posterior distributions represented by finite numbers of particles become narrower than the true distributions. Introducing a lag L, such that α^2 at epoch n is updated every epoch until $n + L$, yields better estimates of the posterior distribution. In other words, $p(\alpha_n^2 | \mathbf{d}_1, \ldots, \mathbf{d}_{n+L}, \ldots \mathbf{d}_k)$, where $k > n + L$, is replaced by $p(\alpha_n^2 | \mathbf{d}_1, \ldots, \mathbf{d}_{n+L})$.

We have found that choosing L too small can fail to detect simulated transients. Spatial under-smoothing has the same result. In contrast, spatial over-smoothing can cause α^2 to be over estimated. To reduce computational complexity one can expand the slip in an orthornomal basis based. One then employs a depleted basis, keeping only the most significant terms in the expansion. This was the approach of Fukuda et al. [2008]. The Kalman filter estimates the time-varying coefficients of the basis functions. We find that it is, however, important to include an appropriate number of basis functions, as illustrated in Figure 4. We address these issues by tracking the normalized data misfit, the norm of the random walk components, and a norm of the estimated slip-rate. The first two measures allow us to protect against over- smoothing which will either misfit the data, or map the misfits into the random walk terms. The latter protects against mapping temporal variations into extreme spatial roughness.

We concluded that for proper imaging and detection of transients it is necessary to account for temporally varying spatial smoothing (regularization of the inverse problem). Specifically, we expect the background slip-rate distribution to be smoother than that during the transient. This necessitates two changes to the algorithm. First, we need to implement spatial smoothing via pseudo-observations rather than through the *prior* covariance matrix. Secondly, each particle in the particle filter must now represent a two-vector (α, γ), where α reflects temporal smoothing (as in the current implementation), and γ reflects spatial smoothing. Work on this was interrupted by the Tohoku earthquake.

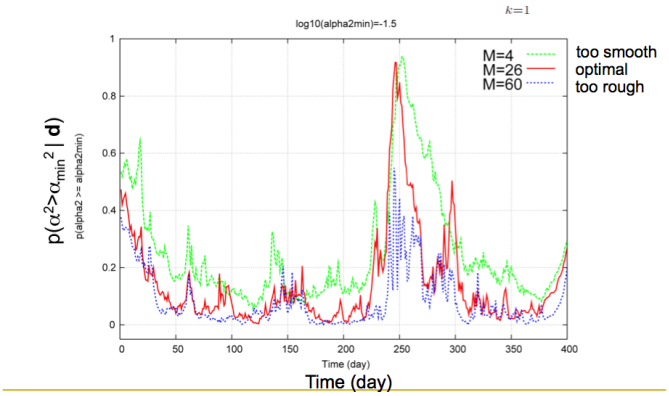

Figure 4: Probability of detecting a transient as a function of time for different numbers of basis functions M. Note that if M is too large the transient probability is diminished, whereas if M is too small, the probability remains high after the transient has actually ceased.

2.2 Network Strain Filter

We (with Jeff McGuire WHOI, and Ryu Ohtani, GSJ, Japan) also developed an alternate set of algorithms referred to as Network Strain Filters [*Ohtani et al.*, 2010]. The approach is to search for spatially coherent transients in the surface strain-rate field. The advantage of this approach is that it is not dependent on a particular fault model. The disadvantage is that, because it is not tied to a physical model, there is no obvious way to separate tectonic from non-tectonic motions. The two approaches, NIF and NSF, are complementary, in that the strain filter may first detect transients, which could be further analyzed with a NIF. In both cases spatial coherence is enforced on the transient signal at the outset. This contrasts with a number of other approaches that analyze the time series at individual stations separately, and then later look to see if the deviations from steady-state are spatially coherent.

As with the NIF and MCMKF we model the data as the sum of steady-state and transient deformations, reference frame and seasonal errors, and local benchmark motions. With the Network Strain Filter, however, we forgo associating transient deformation with specific sources and simply seek a spatially coherent strain-rate field consistent with the GPS data. Expanding $\mathbf{u}_r^{\text{tect}}(\mathbf{x}, t)$ in spatial wavelet basis functions $B_n(\mathbf{x})$ $u_i^{\text{tect}}(\mathbf{x}, t) = \sum_k^K B_k^{(i)}(\mathbf{x}) c_k^{(i)}(t)$

where the index $^{(i)}$ refers to the component of displacement.Assuming a differentiable basis one can compute the strain and rotation from the gradient of the displacement,

$$\frac{\partial u_i^{\text{tect}}(\mathbf{x},t)}{\partial x_j} = \sum_k^K \frac{\partial B_k^{(i)}(\mathbf{x})}{\partial x_j} c_k^{(i)}(t). \tag{4}$$

We assume a separable basis, $B(x,y) = \{\Psi(x) \otimes \Psi(y)\}$ where x and y are latitude and longitude and $\Psi(x)$ represents a one-dimensional wavelet.The Strain Filter estimates the coefficients $c_k^{(i)}(t)$ using a Kalman filter, including random walk, reference frame corrections. We have conducted a number of blind tests comparing results using different wavelet bases. In addition to the transient signal component, the synthetic data included secular motion, as well as colored and white noise (Figure 5). Results are generally positive, although the recovered transient tends to be smeared out in time, a feature of both the NIF and NSF with constant α^2. Including a particle filter as in the MCMKF would alleviate this problem. We developed an appropriate spatial regularization that specifies how the different wavelet scales are weighted. We seek strain-rate distributions that are to some degree spatially smooth. This leads to a Gram matrix (inner product of the basis functions) with entries that scale with the spatial order of the wavelet. In the Kalman filter this scaling is used to weight the a priori covariance matrix as in Segall and Matthews [1997]. The transient terms at all spatial scales are set *a priori* to zero, however the uncertainty in the prior is much less for the smaller spatial scales. Secondly, by estimating the secular deformation with station velocities rather than expanded in basis functions, we minimize the leakage of secular deformation into the inferred transients. The simulation in Figure 5 shows that weak transients can be detected in the presence of colored noise.

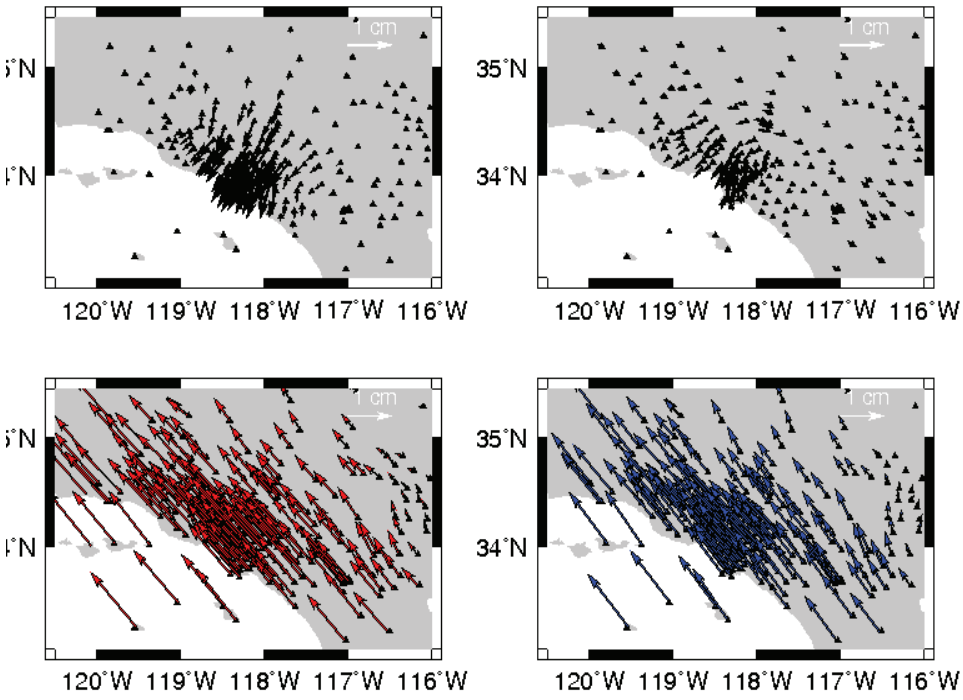

Figure 5: Results of strain filter test (internal blind test prior to SCEC exercise). top left) true transient displacement at final epoch; top right) estimated transient displacement at final epoch; bottom left) True secular velocity field; bottom right) estimated secular velocity field.

References

[1] Fukuda, J., T. Higuchi, S. Miyazaki, and T. Kato (2004), A new approach to time-dependent inversion of geodetic data using a Monte Carlo mixture Kalman filter, *Geophys. J. Int.*, *159*, 17–39, doi:10.1111/j.1365-246X.2004.02383.x.

[2] Fukuda, J., S. Miyazaki, T. Higuchi, and T. Kato (2008), Geodetic inversion for space-time distribution of fault slip with time-varying smoothing regularization, *Geophys. J. Int.*, *173*, 25–48, doi:10.1111/j.1365-246X.2007.03722.x.

[3] Kitagawa, G. (1996), Monte Carlo filter and smoother for non-Gaussian nonlinear state space models, *J. Comput. Graph. Statist.*, *5*, 1–25.

[4] Linde, Alan T., Michael T. Gladwin, Malcolm J. S. Johnston, Ross L. Gwyther, Roger G. Bilham, (1996) A slow earthquake sequence on the San Andreas fault Nature 383, 65-68 (5 September 1996) doi:10.1038/383065a0.

[5] McGuire, J. J., and P. Segall (2003), Imaging of aseismic fault slip transients recorded by dense geodetic networks, *Geophys. J. Int.*, *155*, 778–788, doi:10.1111/j.1365-246X.2003.02022.x.

[6] Miyazaki, S., J. J. McGuire, et al. (2003), A transient subduction zone slip episode in southwest Japan observed by the nationwide GPS array, J. Geophys. Res, 108, 2087.

[7] Miyazaki, S., P. Segall, et al. (2004), Space time distribution of afterslip following the 2003 Tokachi-oki earthquake: Implications for variations in fault zone frictional properties, Geophys. Res. Lett, 31(6).

[8] Miyazaki, S., P. Segall, et al. (2006), Spatial and temporal evolution of stress and slip rate during the 2000 Tokai slow earthquake, J. Geophys. Res, 111.

[9] Murray, J. and P. Segall (2005), Spatiotemporal evolution of a transient slip event on the San Andreas fault near Parkfield, California, *J*ournal of Geophysical Research, v 110,.

[10] Nadeau, R. M., and D. Dolenc (2005), Nonvolcanic tremors deep beneath the San Andreas Fault, *Science*, *307*, 389, doi:10.1126/science.1107142.

[11] Ohtani, R., J. J. McGuire, and P. Segall (2010), The Network Strain Filter - A new tool for monitoring and detecting transient deformation signals in GPS arrays, *J. Geophys. Res.*, doi:10.1029/2010JB007442, in press.

[12] Ozawa, S., M. Murakami, et al. (2005), Transient crustal deformation in Tokai region, central Japan, until May 2004, Earth, Planets, and Space, 57(10), 909-915.

[13] Segall, P., and M. Matthews (1997), Time dependent inversion of geodetic data, *J. Geophys. Res.*, *102*(B10), 22,391–22,409.

[14] Segall, P., R. Bürgmann, and M. Matthews (2000), Time-dependent triggered afterslip following the 1989 Loma Prieta earthquake, *J. Geophys. Res.*, *105*(B3), 5,615–5,634.

[15] Shelly, D. R., Migrating tremors illuminate complex deformation beneath the seismogenic San Andreas fault, Nature 463, 648-652 — doi:10.1038/nature08755

3 Bibliography of publications under SCEC3

Ohtani, R., J.J. McGuire, and P. Segall, (2010),The Network Strain Filter, a new tool for monitoring and detecting transient deformation signals in GPS arrays, J. Geophys. Res., 115, B12418, doi:10.1029/2010JB007442.